

ON THE BEHAVIOUR AND ULTIMATE STRENGTH OF LONGITUDINALLY STIFFENED FLANGES OF STEEL BOX GIRDERS

By Yoshikazu YAMADA and Eiichi WATANABE***

1. INTRODUCTION

The ultimate strength of box girder is controlled mainly by the strengths of the component members, namely, flanges, webs, and bulkheads. This paper presents an investigation on the load carrying capacity of box girders, and concerns itself particularly with the local strength of the stiffened compression flanges. In spite of a great number of researches on this particular subject, not a few problems remain still unsatisfactorily solved.

This program of investigation consists of experimental and theoretical studies performed simultaneously and closely incorporated, in which the behaviour and the ultimate strength of the flange plates are inquired. The investigation aims eventually at some possible representation of the ultimate strength in terms of simple design variables.

The elastic buckling of stiffened plates under uniaxial compression has been well studied since Timoshenko¹⁾ and Barbé^{2),3)}, and has been almost completely investigated by Klöppel, Sheer, and Möller in the case of ribs without substantial torsional rigidity.^{4),5)}

The ultimate strength of unstiffened plates has been studied by von Karman⁶⁾, Timoshenko⁷⁾, Yoshiki⁸⁾, and Dwight⁹⁾. Some of these results have been taken into account in various specifications.^{10),11),12)} Furthermore, the effect of residual stress upon the ultimate strength of unstiffened plate has been studied so well as to be considered in the design of steel bridges of Japan.¹³⁾

The ultimate strength of stiffened plates, however, does not seem to have been studied as

much as the former studies mentioned so far. Among many researches on this subject, Skaloud^{14),15)}, investigated the effect of initial curvature on the post-critical strength and Maquoi¹⁶⁾ performed postbuckling analysis of orthotropic plates by series expansion with special attention to the initial deflection and compared the results with those from Dubas's tests¹⁷⁾; while Ito¹⁸⁾, Ushio¹⁹⁾, Fukumoto²⁰⁾, and Hasegawa²¹⁾ placed emphasis on the effect of the residual stress in the linear buckling analysis; on the other hand, Murray²²⁾,²³⁾ and Sherbourne²⁴⁾ investigated the failure mechanisms of stiffened plates based on the rigid-plastic theory.

In the United Kingdom, an extensive program of study was conducted on this subject by Merison Committee²⁵⁾ after some accidents of box girder bridges and from the results, the Interim Design Rules was made for the design and method of erection of steel box girder bridges. Nevertheless, the interpretation of the Rules is rather difficult and they seem to give quite conservative results²⁶⁾.

The present paper consists of three aspects: The first aspect is devoted to the postbuckling analysis of stiffened plates under uniaxial compression with the extension to the case of elastoplastic stiffeners by finite element method. The second aspect is devoted to the description of the test program conducted at Kyoto University and the results. The third aspect is devoted to the presentation and comparison of available test results at several institutions besides at Kyoto University, from which an empirical formula for the ultimate strength of stiffened plates is derived.

2. EXPERIMENTAL INVESTIGATION

(1) Scope of Study

The purpose of the experimental program is to investigate the load carrying characteristics of

* Dr. Eng., Professor of Kyoto University.

** Ph. D., Assistant Professor of Kyoto University.

with JIS (Japanese Industrial Standards).

Just before the loading test, the initial deflection of the flange plate was measured by automatic level, and during the test, the followings were recorded: readings of the load cells, and the testing machine, deflections of the flange plates, strains of the webs and flange plates.

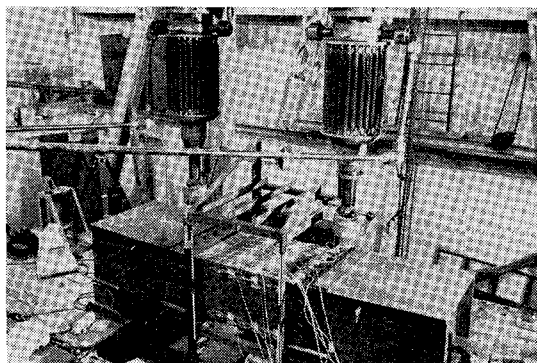


Photo 1 Loading Test of Box Girders.

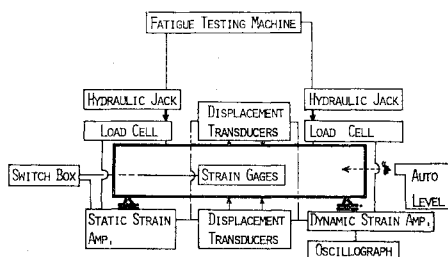


Fig. 3 Instrumentation for Loading Test.

Among those, web strains were recorded to obtain the total compressive force of flange as will be described in the following section, and the deflections of the flange plate were recorded together with the strains of the flange plate and stiffeners mainly to examine the postbuckling characteristics. In other words, the strain readings of the flange plate and stiffeners were analyzed mainly to obtain the change of lateral distribution of both the in-plane and flexural strains in the postbuckling range, and to obtain the load-strain relationships with a view to finding the initiation of plastification of the stiffened plate. A schematic diagram is shown in Fig. 3 to indicate the measurement during the test; while, the instrumentation on the specimen is illustrated by Figs. A.1. and A.2. in the Appendix.

The positions of instrumentation were determined in accordance with the mesh points of FEM analysis.

(3) Evaluation of Flange Force

The measurement of the flange force is one of the most important aspects of the test. The direct method would have required a great number of rosette gages mounted on both surfaces of the flange, which was not actually employed for various difficulties. In the present test an indirect method was employed to get the flange force: This method is based on the measurement of the web strains that are more stable than flange strains. Since the axial stress and the bending stress exerted on the webs can be thought to be linearly distributed across the depth of the webs and are in so-called plane stress condition, the total force carried by the flange can be easily obtained from the equilibrium condition.

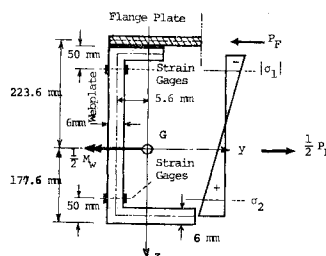


Fig. 4 Axial Stress Distribution of Web.

Fig. 4 shows a portion of the cross section of the box girder, assuming the linear stress distribution, then the stress σ can be obtained in terms of the bending moment carried by two webs, M_w , and the axial compression P_F :

$$\sigma = \frac{I_{zz}z - I_{yz}y}{I_{yy}I_{zz} - I_{yz}^2} \left(\frac{1}{2} M_w \right) + \frac{1}{2} \frac{P_F}{A_w} \quad \dots\dots\dots (1)$$

where I_{zz} and I_{yy} denote the moments of inertia with respect to z and y axis, respectively, and I_{yz} , A_w refer to the product of inertia of the cross section, and the area of a web, respectively.

Substituting specific values to z and y , $|\sigma_1|$ and σ_2 can be expressed in terms of M_w and P_F , and conversely, M_w and P_F can be expressed in the following equations: (both in cm^2)

$$\left. \begin{aligned} M_w &= 294.28(|\sigma_1| + \sigma_2) \\ P_F &= -27.106|\sigma_1| + 30.86\sigma_2 \end{aligned} \right\} \quad \dots\dots\dots (2)$$

3. THEORETICAL INVESTIGATION

(1) Scope of Study

The purpose of the theoretical investigation is

firstly to evaluate the linear buckling load, and secondly to analyze the postbuckling behavior of the stiffened plate while incorporating the results with those from the experimental investigation conducted simultaneously.

(2) Formulation of Problems by FEM²⁷⁾

The element used herein is a rectangular ACM element and can take into account the stiffeners along four edges. It is assumed that the plate itself and the stiffeners are made of homogeneous, isotropic, and elastic materials at first; later on, an extension is made to the case of elasto-plastic stiffeners.

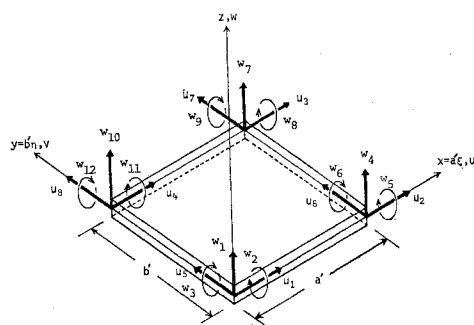


Fig. 5 Rectangular Element.

Fig. 5 shows the rectangular element. Let the displacement components be expressed by u , v , and w , associated with the rectangular coordinates shown in the figure, then, these can be expressed in terms of the nodal displacements, u_i and w_i using dummy indices:

$$u = \alpha_{kl} u_k; \quad v = \alpha_{kl} u_{k+4}; \quad w = \beta_{kl} w_l \quad (k=1, \dots, 4; l=1, \dots, 12) \quad \dots (3)$$

where

$$\alpha_{kl} = a_{km} n_s^{m-1} \gamma_l^{n-1}, \quad \beta_{kl} = b_{kp} q_s^{p-1} \gamma_l^{q-1} \quad (1 \leq m, n \leq 2; 1 \leq p, q \leq 4).$$

Table 1 Components of a_{kij} .

i	j	k			
		1	2	3	4
1	1	1	0	0	0
1	2	-1	0	0	1
2	1	-1	1	0	0
2	2	1	-1	1	-1

The values of a_{kij} and b_{kij} are given in Tables 1 and 2. Let the strain be represented by ε_i , and let the angle of rotation of the stiffener be represented by ϕ , then,

Table 2 Components of b_{kij} .

i	j	k											
		1	2	3	4	5	6	7	8	9	10	11	12
1	1	1	0	0	0	0	0	0	0	0	0	0	0
1	2	0	1	0	0	0	0	0	0	0	0	0	0
1	3	-3	-2	0	0	0	0	0	0	0	3	-1	0
1	4	2	1	0	0	0	0	0	0	0	-2	1	0
2	1	0	0	-1	0	0	0	0	0	0	0	0	0
2	2	-1	-1	1	1	1	0	-1	0	0	1	0	-1
2	3	3	2	0	-3	-2	0	3	-1	0	-3	1	0
2	4	-2	-1	0	2	1	0	-2	1	0	2	-1	0
3	1	-3	0	2	3	0	1	0	0	0	0	0	0
3	2	3	0	-2	-3	0	-1	3	0	1	-3	0	2
3	3	0	0	0	0	0	0	0	0	0	0	0	0
3	4	0	0	0	0	0	0	0	0	0	0	0	0
4	1	2	0	-1	-2	0	-1	0	0	0	0	0	0
4	2	-2	0	1	2	0	1	-2	0	-1	2	0	-1
4	3	0	0	0	0	0	0	0	0	0	0	0	0
4	4	0	0	0	0	0	0	0	0	0	0	0	0

$$\left. \begin{aligned} \varepsilon_i &= B_{ik}^P u_k + \frac{1}{2} B_{ikl}^{PB} w_k w_l + B_{ik}^B w_k; \\ \frac{d\phi}{ds} &= B_{ik}^{\phi} w_k; \quad \frac{d^2\phi}{ds^2} = B_{ik}^{\phi\phi} w_k \end{aligned} \right\} \quad \dots (4)$$

where s represents distance along the stiffeners, and B_{ik}^P , B_{ik}^B , B_{ikl}^{PB} , B_{ik}^{ϕ} , and $B_{ik}^{\phi\phi}$ are referred to as strain functions.

Now, at first, only the elastic behaviour is considered. Let the elastic constants be denoted by D_{ij} , then the following relations hold between the stress and the strain:

$$\sigma_i = D_{ij} \varepsilon_j \quad (j: \text{dummy}) \quad \dots (5)$$

Then, the strain energy stored in the element, U , can be given by

$$\begin{aligned} U &= \sum_i \int_V \int \sigma_i \varepsilon_i dV + \frac{1}{2} \int_s \left\{ GJ_s \left(\frac{d\phi_E}{ds} \right)^2 \right. \\ &\quad + \sigma_s I_{ps} \left(2 \frac{d\phi_I}{ds} + \frac{d\phi_E}{ds} \right) \frac{d\phi_E}{ds} \\ &\quad \left. + EC_{ws} \left(\frac{d^2\phi_E}{ds^2} \right)^2 \right\} ds \quad \dots (6) \end{aligned}$$

where GJ_s , EC_{ws} , and I_{ps} refer to the torsional rigidity, torsional bending rigidity, and the polar moment of inertia of the stiffener, respectively. The subscripts I and E refer to the initial displacement, and the elastic displacement, respectively. The first integral is a volume integral indicating the strain energy of the plate element, and that of the stiffeners corresponding to the axial, and bending deformations. Using the generalized nodal displacements, δ_i ($i=1, \dots, 20$), the strain energy, U , can be rewritten in the following form using dummy indices:

$$\left. \begin{aligned} U &= \frac{1}{2} (K_{ij}^* + S_{ij}^*) \delta_i \delta_j ; \\ (\delta)^T &= (u, \dots, u_8, w_1, \dots, w_{12}) \end{aligned} \right\} \dots\dots(7)$$

$$\left. \begin{aligned} \dot{P}_i &= \frac{\partial P_i}{\partial \delta_j} \dot{\delta}_j = (K_{ij}^{***} + S_{ij}^{***}) \dot{\delta}_j ; \\ \Delta P_i &= (K_{ij}^{***} + S_{ij}^{***}) \Delta \delta_j + R_i^P + R_i^S \end{aligned} \right\} \dots\dots(9)$$

The equations of equilibrium and their incremental equations can also be given by the equations: ("." implies a derivative with respect to some parameter, say, the magnitude of load)

$$P_i = \frac{\partial U}{\partial \delta_i} = (K_{ij}^* + S_{ij}^*) \delta_j ; \dots\dots\dots(8)$$

where P_i refer to the nodal forces, and K_{ij}^* , K_{ij}^{**} , K_{ij}^{***} and S_{ij}^* , S_{ij}^{**} , S_{ij}^{***} refer to the element stiffness matrices of the plate itself and the stiffeners, respectively, being given by the following equations:

$$\left. \begin{aligned} [K^*] &= [K_0] + \frac{1}{3} [K_I] + \frac{1}{6} [K_{II}] ; & [S^*] &= [S_0] + \frac{1}{3} [S_I] + \frac{1}{6} [S_{II}] \\ [K^{**}] &= [K_0] + \frac{1}{2} [K_I] + \frac{1}{3} [K_{II}] ; & [S^{**}] &= [S_0] + \frac{1}{2} [S_I] + \frac{1}{3} [S_{II}] \\ [K^{***}] &= [K_0] + [K_I] + [K_{II}] ; & [S^{***}] &= [S_0] + [S_I] + [S_{II}] . \end{aligned} \right\} \dots\dots\dots(10)$$

in which

$$\left. \begin{aligned} [K_0] &= \left[\begin{array}{c|c} K_{ij}^P & K_{ijk}^{PB} w_k^I \\ \hline K_{jik}^{PB} w_k^I & K_{ij}^B + K_{ijk}^{BB} w_k^I w_l^I \end{array} \right] \\ [K_I] &= \left[\begin{array}{c|c} 0 & K_{ijk}^{PB} w_k^I \\ \hline K_{jik}^{PB} w_k^E & K_{ijk}^{PB} u_k^E + 3K_{ijk}^{BB} w_k^I w_l^E \end{array} \right] \\ [K_{II}] &= \left[\begin{array}{c|c} 0 & 0 \\ \hline 0 & \frac{3}{2} K_{ijk}^{BB} w_k^E w_l^E \end{array} \right] \end{aligned} \right\} \dots\dots\dots(11)$$

$$\left. \begin{aligned} [S_0] &= \left[\begin{array}{c|c} S_{ij}^P & (S_{ijk}^{PB} + S_{ijk}^{\phi}) w_k^I \\ \hline (S_{jik}^{PB} + S_{jik}^{\phi}) w_k^I & S_{ij}^B + S_{ij}^{\phi} + (S_{ijk}^{BB} + \bar{S}_{ijk}^{\phi}) w_k^I w_l^I \end{array} \right] \\ [S_I] &= \left[\begin{array}{c|c} 0 & (S_{ijk}^{PB} + S_{ijk}^{\phi}) w_k^E \\ \hline (S_{jik}^{PB} + S_{jik}^{\phi}) w_k^E & (S_{ijk}^{PB} + S_{ijk}^{\phi}) u_k^E + 3(S_{ijk}^{BB} + S_{ijk}^{\phi}) w_k^I w_l^E \end{array} \right] \\ [S_{II}] &= \left[\begin{array}{c|c} 0 & 0 \\ \hline 0 & \frac{3}{2} (S_{ijk}^{BB} + S_{ijk}^{\phi}) w_k^E w_l^E \end{array} \right] \end{aligned} \right\} \dots\dots\dots(12)$$

and,

$$\bar{S}_{ijk}^{\phi} = S_{jik}^{\phi} + S_{ikj}^{\phi} ; \quad S_{ijk}^{\phi} = \frac{1}{3} (\bar{S}_{ijk}^{\phi} + \bar{S}_{ikj}^{\phi} + \bar{S}_{kij}^{\phi}) \dots\dots\dots(13)$$

$$\left. \begin{aligned} K_{kl}^P &= \int_V D_{mn} B_{mk}^P B_{nl}^P dV & S_{kl}^P &= \sum_S E_s A_s \int_S B_{sk}^P B_{sl}^P ds \\ K_{kl}^B &= \int_V D_{mn} B_{mk}^B B_{nl}^B dV & S_{kl}^B &= \sum_S E_s I_s \int_S B_{sk}^B B_{sl}^B ds \\ K_{ijk}^{PB} &= \int_V D_{mn} B_{mi}^P B_{nj}^B B_{lk}^B dV & S_{ijk}^{PB} &= \sum_S E_s A_s \int_S B_{si}^P B_{sj}^B B_{lk}^B ds \\ K_{ijk}^{BB} &= \int_V D_{mn} B_{mi}^B B_{nj}^B B_{lk}^B dV & S_{ijk}^{BB} &= \sum_S \int_S E_s A_s B_{si}^B B_{sj}^B B_{lk}^B ds \\ S_{kl}^{\phi} &= \sum_S \int_S (G J_s B_{1k}^{\phi} B_{1l}^{\phi} + E C_{sw} B_{2k}^{\phi} B_{2l}^{\phi}) ds \\ S_{ijk}^{\phi} &= \sum_S \int_S E_s I_{sp} B_{si}^P B_{sj}^B B_{lk}^{\phi} ds \\ S_{ijk}^{\phi} &= \sum_S \int_S E_s I_{sp} B_{si}^B B_{sj}^B B_{lk}^{\phi} ds \end{aligned} \right\} \dots\dots\dots(14)$$

Furthermore, R^P and R^S can be given by the following equations:

$$\left. \begin{aligned} [R^P] &= \left[\begin{array}{c} -\frac{1}{2} K_{ij}^{PB} \Delta w_j \Delta w_k \\ K_{ij}^{PB} \Delta w_j \Delta w_k + \frac{3}{2} K_{ij}^{BB} \Delta w_j \Delta w_k w_{l0} \end{array} \right] \\ [R^S] &= \left[\begin{array}{c} \frac{1}{2} (S_{ijk}^{PB} + S_{ijk}^{\phi}) \Delta w_j \Delta w_k \\ (S_{kij}^{PB} + S_{kij}^{\phi}) \Delta u_k \Delta w_j + \frac{3}{2} (S_{ijk}^{BB} + S_{ijk}^{\phi}) \Delta w_j \Delta w_k w_{l0} \end{array} \right] \end{aligned} \right\} \dots\dots\dots (15)$$

where Δw_i and Δu_i refer to the increment of the out-of-plane and in-plane displacement, respectively.

The element stiffnesses can be thus explicitly obtained, and they can be easily combined to get the global stiffnesses.

(3) Extension to the Case of Elasto-Plastic Stiffeners

So far, the discussion has been confined to the case of elastic stiffeners. However, as can be seen from the following discussion, it can be extended to the inelastic case by considering the tangent modulus of the stiffeners.

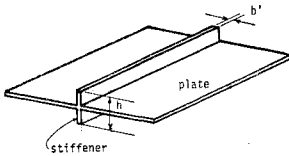


Fig. 6 Plate with Stiffeners in Pair.

Fig. 6 shows a symmetrically spliced stiffener of width b' and depth h . Suppose that it is subjected to the axial force P and the bending moment M , then the following relationships hold from the stress distribution assumed in Fig. 7:

$$\left. \begin{aligned} M &= \frac{b'h^2}{3} (\sigma_Y - \sigma_a) \left(\frac{3}{2} - k \right) \\ \varepsilon_m &= \frac{\sigma_Y}{E} - \left(k - \frac{1}{2} \right) h\kappa \\ P &= \sigma_a b' h \\ k &= \frac{1}{h\kappa} \left(\frac{\sigma_Y}{E} - \varepsilon_m \right) + \frac{1}{2} \\ \kappa &= \frac{2(\sigma_Y - \sigma_a)}{k^2 E h} \end{aligned} \right\} \dots\dots\dots (16)$$

where ε_m , κ , and σ_a refer to the strain at Point C, the curvature, and the average axial stress of the stiffener, respectively. From those, the following relations can be obtained:

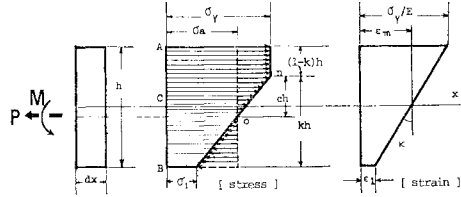


Fig. 7 Stress, and Strain Distribution of Stiffener.

$$\left. \begin{aligned} \frac{\partial M}{\partial \kappa} &= \bar{q}(k) E I_s = \frac{E b' h^3}{12} k(4k^2 - 6k + 3) \\ \frac{\partial \sigma_a}{\partial \varepsilon_m} &= q(k) E = k \\ q(k) &= k ; \quad \bar{q}(k) = k(4k^2 - 6k + 3) \end{aligned} \right\} \dots\dots\dots (17)$$

The physical meaning of $q(k)$ and $\bar{q}(k)$ is explained in Fig. 8.

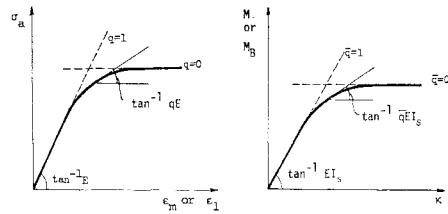


Fig. 8 Tangent Modulus for Axial and Flexural Deformations.

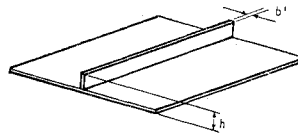


Fig. 9 Plate with a Stiffener Fastened on One Side.

If the stiffener is spliced on one side of the plate as in Fig. 9, the following relations hold similar to those in Eqs. (16) and (17):

$$\left. \begin{aligned} M_B &= M + \frac{b'h^2}{2} \sigma_a; \quad \varepsilon_1 = \frac{\sigma_Y}{E} - kh\kappa \\ \frac{\partial M_B}{\partial \kappa} &= \bar{q}(k)EI_s = \frac{Eb'h^3}{3} k^3 \\ \frac{\partial \sigma_a}{\partial \varepsilon_1} &= q(k)E = kE \end{aligned} \right\} \dots (18)$$

$$q(k) = k; \quad \bar{q}(k) = k^3 \dots (19)$$

Using the tangent modulus functions $q(k)$ and $\bar{q}(k)$, the incremental equations of equilibrium can be given by the equations:

$$\Delta P_i = (K_{ij}^{***} + q'S_{ij}^{***}) \Delta \delta_j + \bar{R}_i^s \dots (20)$$

where q' implies $q(k)$, $\bar{q}(k)$, or similar to those functions, and \bar{R}_i^s is given by the equation:

$$[\bar{R}^s] = \left[\begin{aligned} &\frac{1}{2} (qS_{ij}^{PB} + S_{ij}^{\phi_k}) \Delta w_j \Delta w_k + q'S_{ij}^F \Delta u_j + \frac{1}{2} q'S_{ij}^{PB} \Delta w_j w_{k0} \\ &(S_{ij}^{PB} + S_{ij}^{\phi_k}) \Delta u_k \Delta w_j + \frac{3}{2} (qS_{ij}^{BB_k} + S_{ij}^{\phi_{kl}}) \Delta w_j \Delta w_k w_{l0} + \frac{1}{2} q'S_{ij}^{PB} \Delta u_j w_{k0} + \frac{1}{2} \bar{q}' S_{ij}^B \Delta w_j \\ &+ \frac{1}{2} q'S_{ij}^{PB} \Delta w_j w_{k0} + \frac{3}{4} q'S_{ij}^{BB_k} \Delta w_j w_{k0} w_{l0} - \frac{1}{4} q'S_{ij}^{BB_k} \Delta w_j w_k w_l^I \end{aligned} \right]$$

in which

$$\left. \begin{aligned} q' &= \frac{\partial q}{\partial u_m} \Delta u_m + \frac{\partial q}{\partial w_m} \Delta w_m \\ \bar{q}' &= \frac{\partial \bar{q}}{\partial u_m} \Delta u_m + \frac{\partial \bar{q}}{\partial w_m} \Delta w_m \end{aligned} \right\} \dots (21)$$

(4) Linearization by Means of Perturbation Method

Various numerical techniques have been developed to linearize problems of geometrically and materially nonlinear problems. The classification of the techniques is well summarized and explained in Stricklin's paper²⁸⁾. The selection of the method for use will depend on the accuracy required, the computer time allowed, the degree of nonlinearity, and the ease with which researchers are familiar.

In this paper, perturbation method is selected considering the above-mentioned points²⁸⁾. The perturbation method consists in expanding certain quantities such as the load, deflections, stiffnesses, and strains in terms of some small appropriate parameter into the layered form. Either the increment of the load, ΔP_i , or that of the deflection, $\Delta \delta_i$, of Eq. (20) was selected to be the perturbation parameter. However, the formulation of the problem by means of the perturbation technique may be wholly omitted herein due to the limitation on the pages.

(5) Failure Mechanism of Buckled Flanges

The discussion herein is proceeded using so-called rigid-plastic theory using Tresca's yield criterion³⁰⁾ and assuming the stiffened plate remaining plane prior to the attainment of the ultimate load, and it is limited to the cases of upto two stiffeners. The failure mechanism considered herein consists of flat planes and plastic

hinges about which the rigid planes rotate.

In case there is no stiffener or a single stiffener, the mechanism may be given by Fig. 10 provided that the loaded edges are clamped and the unloaded edges are simply supported. A simple energy consideration will lead to the following load-deflection relationship, or in other words, unloading curve:

$$Pw = 2M_p(a \tan \phi + 2b) + 4M_{ps} \dots (22)$$

where M_p , and M_{ps} refer to the plastic moment of the plate, and the stiffener, respectively.

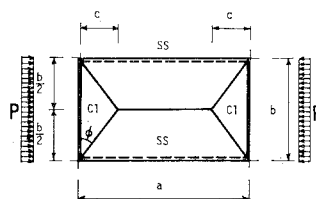


Fig. 10 Yield Lines of Plate with a Single Rib.

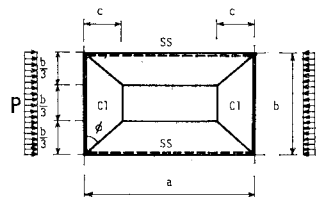


Fig. 11 Yield Lines of Plate with Two Ribs.

In case of no or two stiffeners spaced at equal intervals, the failure mechanism may be as given by Fig. 11 assuming the same boundary condition as before. Then the following relationship will be obtained similar to Eq. (22).

$$Pw = \frac{\tan \phi}{1 + \tan \phi} b M_p \left(3 \frac{a}{b} - 2 \tan \phi + \frac{4}{\tan \phi} + \frac{4}{\sin 2\phi} \right) + 12 \frac{M_{ps}}{1 + \tan \phi} \dots (23)$$

The effect of the axial compressive force, P , and the crash load, P_p , have been neglected in Eqs. (22) and (23). Although the rigorous derivation is difficult, the effect of the axial force may be approximately considered in the above equations if M_p and M_{ps} are replaced respectively by $M_p[1 - (P/P_p)^2]$ and $M_{ps}[1 - (P/P_p)^2]$.

Table 3(a) Dimensions, Cross Sectional and Mechanical Properties of Tested Box Specimens.

Test No.	No. of Stiffeners N	Height of Stiffeners h (mm)	Magnitude of Initial Defl. w_m (mm)	Length of Plate a (mm)	Depth of Plate b (mm)	Thickness of Plate t (mm)	Yielding Stress σ_Y (kg/cm ²)	Thickness of Stiff b' (mm)	Yielding Stress σ_{Ys} (kg/cm ²)
Case 0	0	—	3.9	718	600	2.3	2 442	3.0	3 243
Case 1	1	12	1.8						
Case 2	1	15	1.3						
Case 3	1	19	1.3						
Case 4	2	14	1.8						
Case 5	2	18	1.6						
Case 6	2	23	3.7						

Table 3(b) Non-dimensionalized Area and Rigidities of A Stiffener.

Test No.	$\frac{A_s}{bt}$	$r = \frac{EI_s}{bD}$	$\frac{1}{2(1+\nu)} \left(\frac{J_s}{at^3} \right)$
Case 0	0	0	0
Case 1	0.063	3.99	0.0115
Case 2	0.070	6.89	0.0127
Case 3	0.078	12.83	0.0143
Case 4	0.067	5.79	0.0123
Case 5	0.076	11.10	0.0139
Case 6	0.087	21.66	0.0158

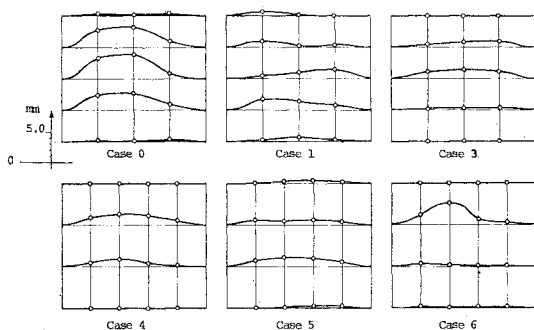


Fig. 12 Observed Initial Deflections of Flange Plates.

the flange, and of the stiffeners to the flange of each specimen. Thus, it may be reasonable to consider the loaded edges of the tested flange plate clamped, and the unloaded edges simply supported.

4. RESULTS AND DISCUSSIONS

(1) General Remarks

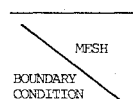
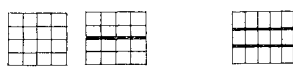
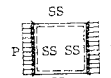
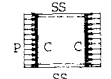
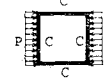
The dimensions, cross sectional and mechanical properties of seven tested box girders are shown in Table 3. Each of the tested box specimens were bolted tightly along the webs and flange to those of the end beams; while spot welding was adopted for the connection of the webs to

As shown in Table 3, the yielding strength of thin plates used for the flanges of thickness 2.3 mm averaged 2 440 kg/cm², which was much less than that for the stiffeners of thickness 3.0 mm averaged 3 240 kg/cm².

The observed initial deflections of the tested flange plates are shown in Fig. 12. The maximum values varied from 60% to 170% of the thickness of the plates.

The theoretical computation consists of the eigen value analysis and nonlinear postbuckling analysis. Perturbation method was exclusively used for the linearization of the problem since

Table 4 Mesh and Degree of Freedom in Finite Element Analysis.

				
			86	81
			80	77
			74	69

it was found through preliminary computations, the results by Newton-Raphson's method did not yield too much difference from those by perturbation method of second order for appropriate interval of incremental steps.

The mesh employed in FEM analysis is shown in Table 4, and the corresponding degrees of freedom are also shown herein. The size of the mesh was determined in consideration of the

computer time required for fulfilment of each nonlinear analysis. Furthermore, the actual eccentric stiffeners as in Fig. 9 were replaced by the equivalent symmetrically placed ones having the same flexural rigidity and cross-sectional area as in Fig. 6 to avoid complexity in postbuckling analysis; otherwise, more element stiffness matrices in addition to those in Eq. (14) should have been used.

Table 5 Buckling, Yielding, and Ultimate Loads in Tons.

MESH							
SUPPORT CONDITION							
	CASE 0	CASE 1	CASE 2	CASE 3	CASE 4	CASE 5	CASE 6
SS							
P SS SS	P_{cr} 1.49 (1.59)	3.37 (3.50)	4.67 (4.75)	6.12 (6.51)	5.89 (5.92)	9.86 (9.90)	12.13
SS					12.26	16.53	21.52
					12.30	15.99	21.97
SS							
P C C	P_{cr} 2.09 (2.25)	6.71	6.79	6.90	11.17	11.61	12.14
SS	P_Y 4.09	7.27	8.81	9.62	11.98	16.63	16.63
	P_u 5.62	7.27	9.47	9.62	12.32	16.63	22.04
C							
P C C	P_{cr} 3.33 (3.84)	8.77	8.88	9.02	18.33	19.55	20.93
C	P_Y 6.24	10.02	10.86	10.07	14.16	16.00	16.67
	P_u		11.45	10.07			
EXPERIMENTAL ULTIMATE LOAD	6.1	7.7	8.3	9.7	12.3	16.9	19.8

(2) Buckling Loads and Ultimate Loads

The buckling, yielding, and ultimate loads obtained by FEM analysis are shown in Table 5, together with the ultimate loads obtained experimentally. Buckling Loads obtained by Timoshenko's series expansion⁷⁾ are indicated by figures in parenthesis. The yielding load refers to the load at which the yielding initiates in the stiffeners except for Case 0: In Case 0, it refers to the load at which the yielding of unstiffened plate initiates along the loaded edges.

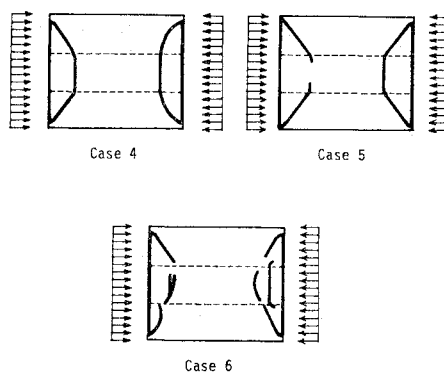
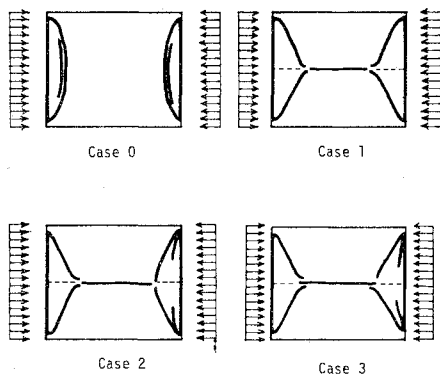


Fig. 13 Sketches of Buckled Flanges.

The ultimate load refers to the load at which either the yielding initiates in the plate element or the deflection of the plate element increases unlimitedly.

The failure mechanisms of the tested flanges are sketched in Fig. 13 and photographed in Photos 2, 3, and 4. Accordingly, the actual plastic hinge lines can be seen well represented by those illustrated in Figs. 10 and 11.

It has been shown that the flange compression,

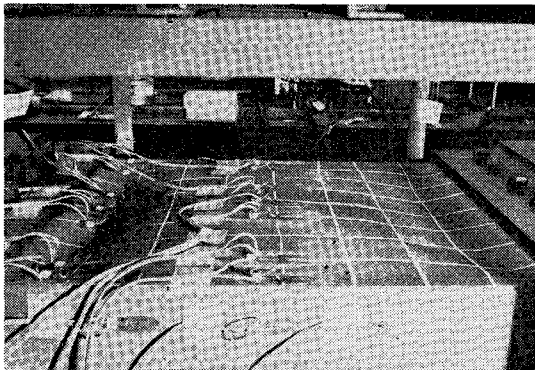


Photo 2 Failure of Flange Plate. Case 0.

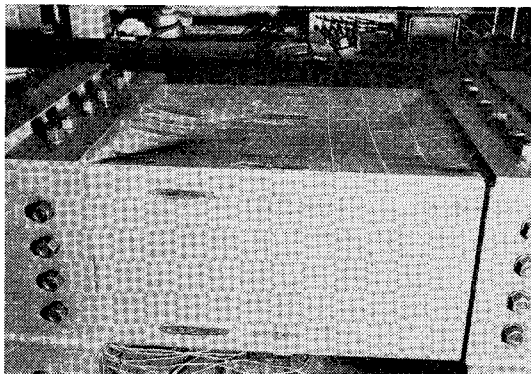


Photo 3 Failure of Flange Plate. Case 1.

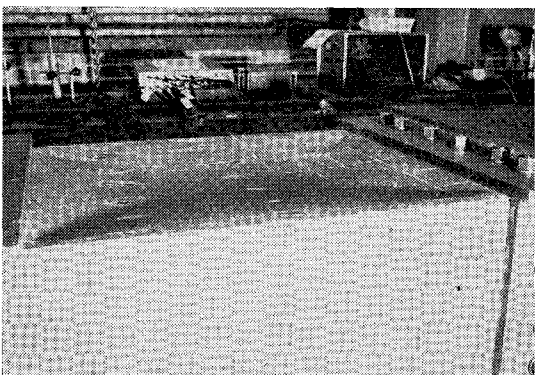


Photo 4 Failure of Flange Plate. Case 5.

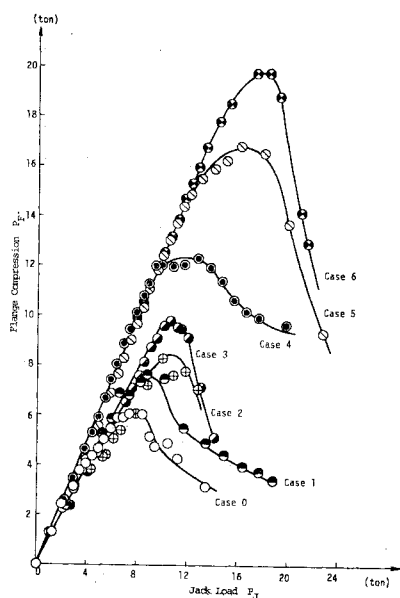


Fig. 14 Flange Force and Jack Load.

P_F , can be obtained through Eq. (2); on the other hand, however, it must also satisfy the moment equilibrium (see Fig. 4). Let P'_F be defined by

$$P'_F = \frac{1}{22.36} (M_T - M_w), \dots\dots\dots (24)$$

where M_T refers to the total bending moment acting on the whole cross section; then, P'_F is seen to satisfy the moment equilibrium.

Provided that the stresses $|\sigma_1|$ and σ_2 were exactly correct, then, P'_F in Eq. (24) should be equal to P_F in Eq. (2). Actually, this is not the case, and the error is always involved. Now let $|\sigma_1|$ be thought to be correct and P_{Fm} be such that

$$P_{Fm} = \frac{1}{2} (P'_F + P_F), \dots\dots\dots (25)$$

and let σ_2^* be chosen instead of the measured stress, σ_2 , so that both Eqs. (2) and (24) be satisfied simultaneously by setting $P'_F = P_F$, then, the corresponding load, P_F^* , may be thought very close to the true load. Consequently, the error

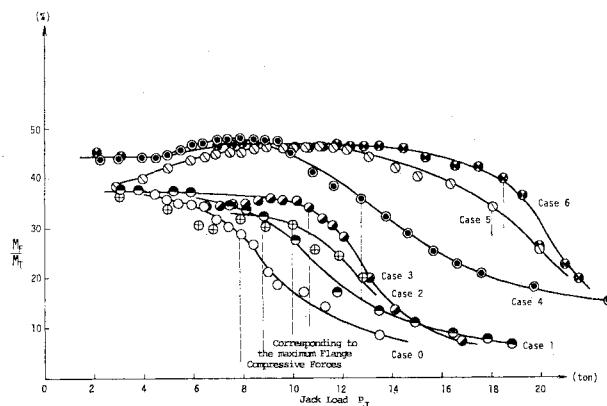


Fig. 15 Ratio of the Bending Moment Carried by the Compression Flange.

involved in the evaluation of the flange force, P_F , may be predicted by the following equation:

$$E_r(P_F) = \frac{P_{Fm} - P_F^*}{P_{Fm}} = \frac{-0.539P_J - 2.8|\sigma_1| + 8.85\sigma_2}{1.34P_J - 15.13|\sigma_1| + 8.6\sigma_2}, \dots (26)$$

where, P_J refers to the magnitude of jack load. The error evaluated at the ultimate load in accordance with Eq. (26) is tabulated in Table 6 for each of the tested box specimens.

The relationship between the flange force and the jack load obtained experimentally for each of the tested girders is given in Fig. 14. Moreover, the ratio of the bending moment carried by the compression flange to the total bending moment exerted by jack loads is also given in Fig. 15, for each of the tested girders.

Table 6 Estimation of Error in Evaluation of Ultimate Flange Compressive Force for Tested Box Specimens.

Case No.	Jack Load P_J (ton)	Flange Compressive Forces				Error $E_r(P_{Fu})$ (%)
		P_{Fu} (ton)	P_{Fu}^* (ton)	P_{Fum} (ton)	P_{Fu}^* (ton)	
1	8.78	8.00	7.25	7.63	7.48	+2.0
2	10.00	8.92	7.63	8.28	8.19	+1.0
3	10.62	10.01	9.46	9.74	10.04	-3.1
4	12.74	11.34	13.27	12.31	12.42	-0.9
5	16.19	16.46	17.26	16.86	16.96	-0.6
6	18.49	19.55	20.03	19.79	19.91	-0.6

(3) Load-Deflection Relationship

The deflections of flange plates were obtained experimentally using electric displacement transducers by subtracting the displacement component corresponding to the rigid body motion

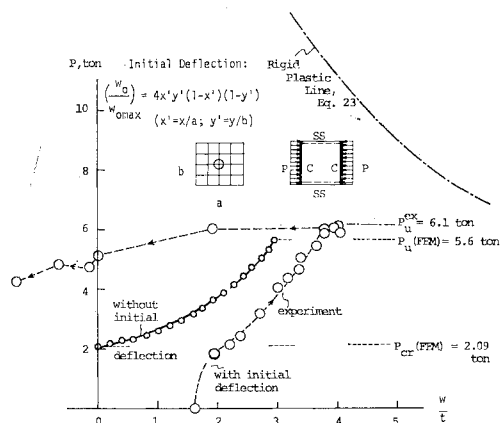


Fig. 16 Load-Deflection Curve. Case 0. (Unstiffened Plate).

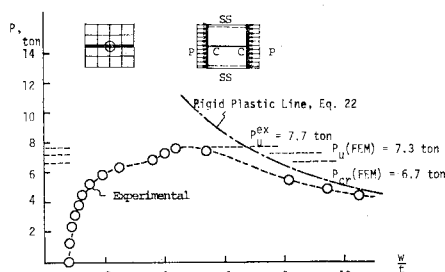


Fig. 17 Load-Deflection Curve. Case 1.

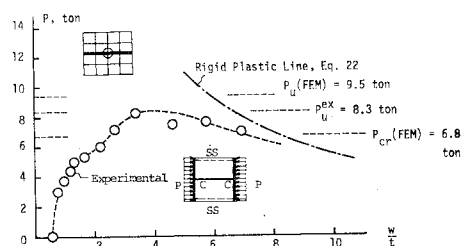


Fig. 18 Load-Deflection Curve. Case 2.

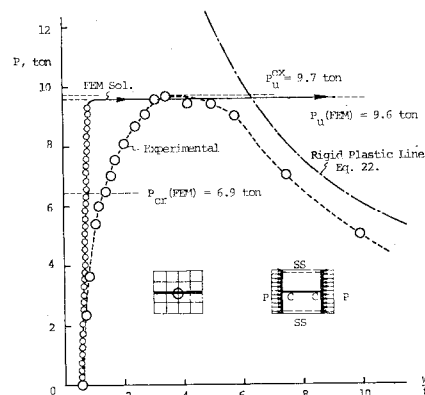


Fig. 19 Load-Deflection Curve. Case 3.

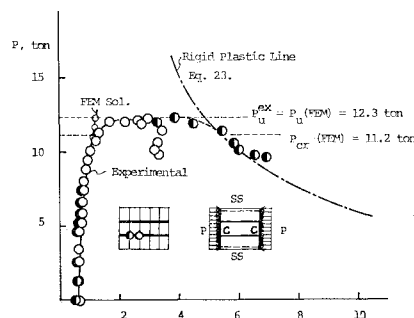


Fig. 20 Load-Deflection Curve. Case 4.

of the box girders. The load-deflection curves of the tested flange plates obtained in this way are shown in Figs. 16 through 22. The results from the postbuckling analysis, and those from the proposed failure mechanisms, Eqs. (22) and (23) are also plotted. In every case, the ultimate load is seen to exceed the linear buckling load, and most of the flange plates underwent the typical postbuckling deflection that is characterized by the portion of load deflection curve convex downward before the ultimate load is reached. Furthermore, every stiffened flange plate demonstrated the existence of the collapse mechanism by the portion of the load-deflection curve convex downward after the ultimate load is reached. It may be interesting to note that a snap-through took place during the test of unstiffened plate. Apparently, in this case, the full plastic capacity was not attained in the collapse.

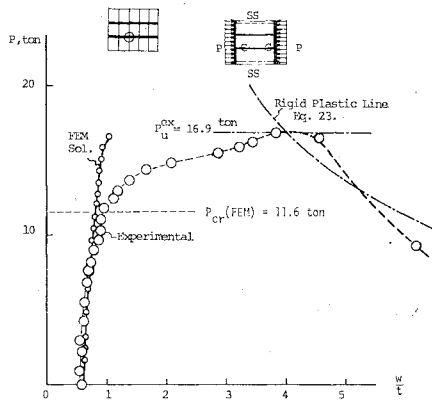


Fig. 21 Load-Deflection Curves. Case 5. (stiffened plate with 2 stiffeners).

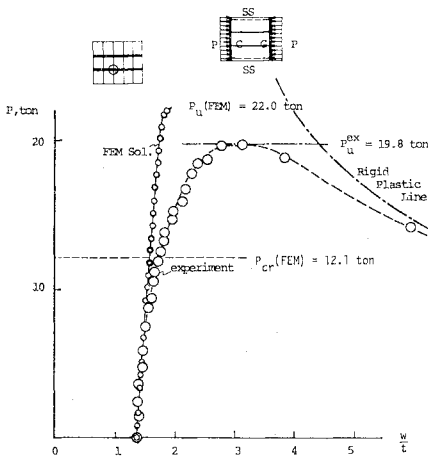


Fig. 22 Load-Deflection Curves. Case 6. (stiffened plate with 2 stiffeners).

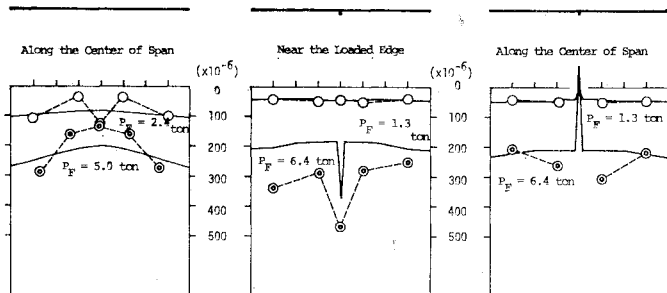


Fig. 23 Axial Strain. Case 0.

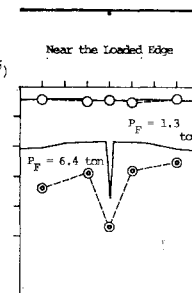


Fig. 24(a) Axial Strain. Case 1.

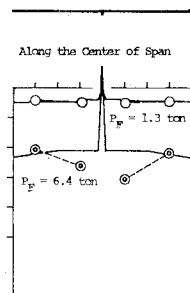


Fig. 24(b) Axial Strain. Case 2.

On the other hand, as can be seen from Table 5, the theory predicted the snap-through type of failure of Case 1 and Case 3: In these cases, the stiffened flange plates deflected unlimitedly at the ultimate load.

(4) Linear Buckling Loads and Deflectional Modes

The linear buckling loads of the tested flange plates have been presented in Table 5, and the failure deflectional modes have been shown in Fig. 13. In this section, the buckling load corresponding to the lowest symmetric mode is considered since the ultimate deflectional shape is always symmetric for each of the tested flange plates. Table 7 shows first few buckling loads of the tested flange plates, and the lowest symmetric modes are indicated by underlines.

Table 7 First Few Buckling Loads of Tested Flange Plates Obtained by FEM.

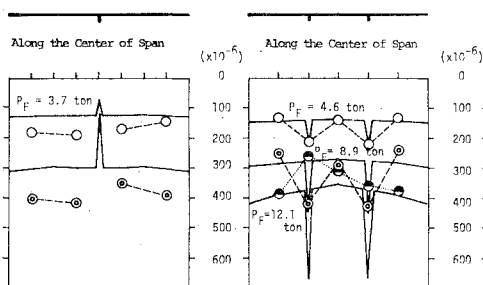
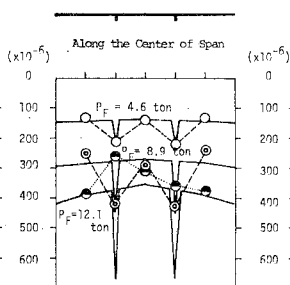
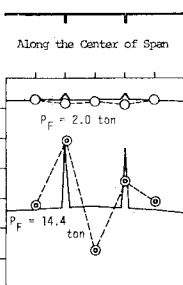
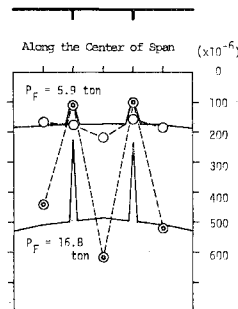
Case No.	Buckling Loads in tons						Exp. Ult. Load in tons
	1st	2nd	3rd	4th	5th	6th	
0	<u>2.09</u>	2.88	4.81	5.92	6.04	8.66	6.14
1	6.71	6.88	<u>7.01</u>	7.66	10.30	11.68	7.63
2	6.79	6.96	<u>7.65</u>	8.07	11.78	12.29	8.28
3	6.90	7.06	<u>7.97</u>	8.38	11.92	12.69	9.74
4	11.17	12.92	14.03	16.82	19.41	27.44	12.31
5	11.61	<u>13.42</u>	14.61	18.08	23.41	31.60	16.86
6	12.14	13.92	15.28	<u>19.04</u>	24.29	34.34	19.79

It would be seen from this table that the ultimate load can not necessarily be given by the linear buckling load even if the appropriate mode is taken.

(5) Distribution of Axial Strain of Flange

The axial strains of the tested flange plates were measured using linear electric resistance strain gages and were compared with those predicted by finite element analysis.

Figs. 23 through 28 show the average axial


 Fig. 25 Axial Strain.
Case 3.

 Fig. 26 Axial Strain.
Case 4.

 Fig. 27 Axial Strain.
Case 5.

 Fig. 28 Axial Strain.
Case 6.

strain distribution of stiffened plates, and wherever the stiffeners are located, the average is taken over the whole cross section including the stiffener. (circles represent the test results.)

5. EMPIRICAL FORMULA

(1) General Remarks

Many formulas have been proposed to represent explicitly the ultimate strength of compressed unstiffened plates.^{8),9),10),11),12)} For instance, according to the AISC specifications¹⁰⁾, the non-dimensionalized ultimate stress, or the ratio of the effective width, can be given by the equation:

$$\left. \begin{aligned} \frac{\sigma_{u0}}{\sigma_Y} &= \frac{b_e}{b} = \frac{1.69}{B} \\ B &= \frac{b}{t} \sqrt{\frac{\sigma_Y}{E}} \end{aligned} \right\} \dots\dots\dots (27)$$

where b , b_e , E , and t refer respectively, the width of the plate, effective width, elastic modulus, and the thickness of the plate. Moreover, σ_{u0} and σ_Y refer to the ultimate stress and the yielding stress of the unstiffened plate, respectively.

On the other hand, none of such simple formulas have been proposed on the ultimate strength of compressed stiffened plates. Thus, in this paper, the explicit representation of the ultimate strength of the stiffened plates is proposed based on the results of tests conducted at various institutions^{17),19),20),21),31),32)} besides those at Kyoto University. This formula is restricted currently to the case of stiffened plates with equal stiffeners without substantial torsional rigidity; nevertheless, it might be easily extended to other cases with appropriate modifications.

(2) Derivation of Formula

If the compressive force were carried by the independent actions of the plate itself and the

stiffeners, the following equation would hold:

$$\left. \begin{aligned} \frac{\sigma_u}{\sigma_Y} &= \frac{1+N\delta r_s}{1+N\delta} \frac{P_u}{P_Y} = \frac{\sigma_{u0}}{\sigma_Y} + \frac{\sigma_{us}}{\sigma_Y} r_s N \delta \\ r_s &= \frac{\sigma_{Ys}}{\sigma_Y} ; \quad \delta = \frac{A_s}{bt} \end{aligned} \right\} (28)$$

where A_s and N refer to the cross sectional area and the number of stiffeners; moreover, P_u and P_Y refer to the ultimate load and the full plastic load of the stiffened plate; whereas σ_{u0} , σ_{us} , and σ_{Ys} refer to the ultimate stress of the stiffened plate, that of the stiffeners, and the yielding stress of the stiffeners, respectively. The first term in Eq. (28) represents the fraction of stress carried by the unstiffened plate; whereas, the second term represent the fraction of stress carried by the stiffeners only.

In actual situation, however, this is not the case. The stress carried by the plate portion is enhanced by the stiffeners' cross sectional area; while the stress carried by the stiffeners depends upon the stiffeners' cross sectional area and the flexural stiffness. Thus, the ultimate strength of the stiffened plates under compression may be represented by the following formula in consideration of Eq. (27):

$$\left. \begin{aligned} \frac{\sigma_u}{\sigma_Y} &= \sqrt{1+2N\phi} \frac{1.69}{B} \\ &+ \frac{\phi}{1+\phi} \sqrt{N \frac{\gamma}{\gamma^*}} \left(N \frac{\gamma}{\gamma^*} \leq 1 \right) \end{aligned} \right\} \dots\dots\dots (29)$$

$$\phi = r_s N \delta ; \quad \gamma = \frac{EI_s}{bD}$$

where γ and γ^* refer to the relative flexural rigidity of a stiffener, and the optimum relative flexural rigidity of a stiffener according to DIN 4114³³⁾, respectively. Furthermore, EI_s and D refer to the flexural rigidity of a stiffener, and the flexural stiffness of plate, respectively.

The results of tests are correlated with those from Eq. (29) in Tables 8, 9, and 10.

Table 8 Ultimate Strength of Stiffened Flange Plate in Compression as Compared with Experimental Value.

TESTS	No. OF RIBS	δ	γ/γ^*	$B - \frac{b}{t} \sqrt{\frac{\sigma_u}{E}}$	$\frac{1.69}{B} \sqrt{\frac{1.69}{E}}$	$\phi = r_s N \delta$	$\sqrt{1 + 2N\delta} \frac{1.69}{B}$	$\frac{\phi}{1 + \phi} \sqrt{N/\gamma^*}$	$\frac{\sigma_u/\sigma_{cr}}{E_{cr}(29)}$	Exp.
Kyoto Univ.	Case 0	0	0	8.893	0.190	0	0.190	0	0.190	0.182
	Case 1	1	0.063	0.365	8.893	0.190	0.084	0.047	0.252	0.205
	Case 2	1	0.070	0.621	8.893	0.190	0.092	0.207	0.067	0.222
	Case 3	1	0.078	1.137	8.893	0.190	0.104	0.209	0.094	0.270
	Case 4	2	0.067	0.300	8.893	0.190	0.179	0.249	0.117	0.313
	Case 5	2	0.076	0.562	8.893	0.190	0.202	0.256	0.168	0.419
Ref. 31	Case 6	2	0.087	1.067	8.893	0.190	0.231	0.264	0.188	0.480
	TPA 2	3	0.15	11.1	7.782	0.217	0.45	0.418	0.310	0.677
	TPA 4	3	0.15	11.1	7.443	0.227	0.45	0.437	0.310	0.747
	TPH 2	3	0.15	11.1	7.950	0.213	0.45	0.410	0.310	0.720
	TPH 4	3	0.15	11.1	7.608	0.222	0.45	0.427	0.310	0.737
	TPC 3	3	0.15	11.1	7.378	0.229	0.45	0.441	0.310	0.751
	TPA 1	4	0.15	7.9	7.367	0.229	0.6	0.551	0.375	0.899
	TPA 3	4	0.15	7.9	7.521	0.225	0.6	0.542	0.375	0.917
	TPB 1	4	0.15	7.9	7.378	0.229	0.6	0.551	0.375	0.926
	TPB 3	4	0.15	7.9	7.795	0.217	0.6	0.523	0.375	0.898
	TPC 2	4	0.15	7.9	7.470	0.226	0.6	0.544	0.375	0.919
	TPC 1	5	0.15	6.0	7.405	0.228	0.75	0.665	0.428	1.093
Ref. 19	TPC 4	5	0.15	6.0	7.544	0.224	0.75	0.653	0.428	1.081
	I	1	0.225	1.022	2.818	0.600	0.225	0.722	0.184	0.906
	II	1	0.225	1.022	2.818	0.600	0.225	0.722	0.184	0.906
	III	1	0.225	1.022	2.818	0.600	0.225	0.722	0.184	0.906

Table 9 Ultimate Strength of Stiffened Flange Plate in Compression as Compared with Experimental Value.

TESTS	No. OF RIBS	δ	γ/γ^*	$B - \frac{b}{t} \sqrt{\frac{\sigma_u}{E}}$	$\frac{1.69}{B} \sqrt{\frac{1.69}{E}}$	$\phi = r_s N \delta$	$\sqrt{1 + 2N\delta} \frac{1.69}{B}$	$\frac{\phi}{1 + \phi} \sqrt{N/\gamma^*}$	$\frac{\sigma_u/\sigma_{cr}}{E_{cr}(29)}$	Exp.
Ref. 32	No. 1	0	0	0	1.04	1.00	0	1.00	1.00	1.13
	No. 2	0	0	0	1.45	1.00	0	1.00	1.00	0.91
	No. 3	1	0.080	0.220	2.07	0.817	0.040	0.880	0.023	0.903
	No. 4	1	0.117	0.888	2.90	0.583	0.117	0.648	0.098	0.746
	No. 5	2	0.063	0.049	1.87	0.903	0.125	1.106	0.035	1.141
	No. 6	2	0.115	0.224	3.11	0.544	0.229	0.753	0.124	0.877
	No. 7	2	0.252	0.918	4.36	0.383	0.505	0.674	0.336	1.010
	No. 8	2	0.186	0.991	6.47	0.262	0.359	0.409	0.264	0.673
	No. 9	2	0.132	0.446	3.24	0.512	0.264	0.734	0.197	0.931
	No. 10	2	0.229	1.007	3.24	0.512	0.482	0.876	0.325	1.150
	No. 11	2	0.252	0.918	4.54	0.372	0.647	0.705	0.393	1.098
	No. 12	2	0.337	1.437	4.54	0.372	0.636	0.700	0.389	1.089
	No. 13	2	0.474	2.116	4.54	0.372	0.798	0.713	0.445	1.150
	No. 14	3	0.087	0.051	2.46	0.687	0.260	1.099	0.080	1.150
	No. 15	3	0.192	0.183	4.10	0.412	0.449	0.792	0.230	1.022
Ref. 21	62-20	1	0.118	0.57	2.21	0.785	0.118	0.850	0.080	0.930
	62-44	1	0.153	1.07	2.19	0.772	0.153	0.882	0.133	1.015
	62-70	1	0.217	1.36	2.19	0.772	0.179	0.899	0.152	1.051
	76-30	1	0.109	0.78	2.78	0.608	0.109	0.671	0.087	0.758
	76-42	1	0.153	0.90	2.74	0.617	0.126	0.690	0.106	0.797
	76-63	1	0.181	1.35	2.74	0.617	0.149	0.703	0.130	0.833
	93-30	1	0.131	0.92	3.56	0.475	0.108	0.523	0.093	0.617
	93-39	1	0.144	1.16	3.59	0.471	0.119	0.524	0.106	0.630
	93-59	1	0.161	1.56	3.63	0.456	0.133	0.524	0.117	0.641
	93-117	1	0.194	2.38	3.42	0.494	0.161	0.568	0.136	0.706
	93-196	1	0.225	3.49	3.42	0.494	0.186	0.579	0.157	0.736
	93-273	1	0.253	4.48	3.44	0.491	0.209	0.585	0.173	0.758
Ref. 20	93-39-A	1	0.142	1.18	3.52	0.480	0.120	0.535	0.107	0.790
	93-59-A	1	0.162	1.61	3.52	0.480	0.136	0.542	0.120	0.662
	93-39-T	1	0.131	0.83	3.42	0.494	0.131	0.555	0.109	0.661
	93-59-T	1	0.161	1.24	3.40	0.497	0.161	0.572	0.139	0.710
	93-30-P	1	0.123	0.77	3.84	0.440	0.088	0.477	0.071	0.548
	93-39-P	1	0.141	1.16	3.52	0.480	0.119	0.534	0.106	0.641
	93-59-P	1	0.153	1.43	3.39	0.499	0.130	0.560	0.115	0.675
	93-1177P	1	0.196	2.44	3.84	0.440	0.139	0.498	0.122	0.620
	C2-90-1	2	0.333	1.17	3.048	0.554	0.672	1.065	0.402	1.467
	C2-120-1	2	0.245	1.04	4.035	0.419	0.499	0.725	0.333	1.058
	C2-120-1A	2	0.250	1.10	4.111	0.411	0.507	0.715	0.336	1.052
	C2-120-1H	2	0.271	1.13	4.375	0.386	0.733	0.766	0.423	1.188
	C2-150-1	2	0.230	1.08	4.999	0.338	0.513	0.590	0.339	0.929
	B-1-1	3	0.075	0.917	5.087	0.332	0.225	0.509	0.184	0.693
	B-1-1r	3	0.083	1.05	5.449	0.310	0.249	0.489	0.199	0.688
	B-1-2	3	0.095	1.65	5.190	0.326	0.285	0.537	0.222	0.759
Ref. 17	B-2-1	3	0.078	0.797	4.646	0.364	0.234	0.564	0.190	0.754
	B-2-4	3	0.164	3.12	4.531	0.373	0.492	0.742	0.330	1.072
	B-3-1	3	0.077	0.45	3.510	0.481	0.231	0.743	0.188	0.931
	C-1-1	4	0.068	1.24	7.436	0.227	0.272	0.465	0.214	0.619
	C-1-2	4	0.087	3.92	7.482	0.226	0.348	0.440	0.258	0.698
	C-1-4	4	0.150	5.08	7.324	0.231	0.600	0.556	0.375	0.931
	C-2-1	4	0.071	1.14	6.645	0.234	0.284	0.459	0.221	0.680
	C-2-2	4	0.087	1.94	6.634	0.255	0.348	0.496	0.258	0.753
	C-2-4	4	0.153	4.33	6.667	0.253	0.614	0.614	0.360	0.994
	M-1	7	0.050	0.424	17.338	0.0975	0.329	0.231	0.248	0.479
Ref. 17	M-2	7	0.070	0.942	17.338	0.0975	0.528	0.282	0.346	0.628
	M-3	7	0.105	1.741	17.338	0.0975	0.742	0.329	0.426	0.755

Table 10 Ultimate Strength of Stiffened Flange Plate in Compression as Compared with Experimental Value.

TESTS	No. OF RIBS	δ	γ/γ^*	$B - \frac{A}{t} \sqrt{\frac{\sigma_u}{E}}$	$\frac{1.69}{B} \sqrt{\frac{1.69}{E}}$ (≤ 1.0)	$\phi - r_s N \delta$	$\sqrt{1 + 2N\delta} \frac{1.69}{B}$ (≤ 1.0)	$\frac{\phi}{1 + \phi} \sqrt{N/\gamma^*}$	$\frac{\sigma_u/\sigma_{cr}}{F_{cr}(29)}$	Exp.	
Ref. 21	93-39-A	1	0.142	1.18	3.52	0.480	0.120	0.535	0.107	0.642	0.790
	93-59-A	1	0.162	1.61	3.52	0.480	0.136	0.542	0.120	0.662	0.793
	93-39-T	1	0.131	0.83	3.42	0.494	0.131	0.555	0.106	0.661	0.722
	93-59-T	1	0.161	1.24	3.40	0.497	0.161	0.572	0.139	0.710	0.754
	93-30-P	1	0.123	0.77	3.84	0.440	0.088	0.477	0.071	0.548	0.700
	93-39-P	1	0.141	1.16	3.52	0.480	0.119	0.534	0.106	0.641	0.701
	93-59-P	1	0.153	1.43	3.39	0.499	0.130	0.560	0.115	0.675	0.740
	93-1177P	1	0.196	2.44	3.84	0.440	0.139	0.498	0.122	0.620	0.697
	C2-90-1	2	0.333	1.17	3.048	0.554	0.672	1.065	0.402	(1.467)	1.061
	C2-120-1	2	0.245	1.04	4.035	0.419	0.499	0.725	0.333	1.058	0.929
	C2-120-1A	2	0.250	1.10	4.111	0.411	0.507	0.715	0.336	1.052	1.049
	C2-120-1H	2	0.271	1.13	4.375	0.386	0.733	0.766	0.423	1.188	1.100
C2-150-1	2	0.230	1.08	4.999	0.338	0.513	0.590	0.339	0.929	0.885	
Ref. 20	B-1-1	3	0.075	0.917	5.087	0.332	0.225	0.509	0.184	0.693	0.831
	B-1-1r	3	0.083	1.05	5.449	0.310	0.249	0.489	0.199	0.688	0.835
	B-1-2	3	0.095	1.65	5.190	0.326	0.285	0.537	0.222	0.759	0.903
	B-2-1	3	0.078	0.797	4.646	0.364	0.234	0.564	0.190	0.754	0.841
	B-2-4	3	0.164	3.12	4.531	0.373	0.492	0.742	0.330	1.072	1.061
	B-3-1	3	0.077	0.45	3.510	0.481	0.231	0.743	0.188	0.931	0.997
	C-1-1	4	0.068	1.24	7.436	0.227	0.272	0.465	0.214	0.619	0.719
	C-1-2	4	0.087	3.92	7.482	0.226	0.348	0.440	0.258	0.698	0.746
	C-1-4	4	0.150	5.08	7.324	0.231	0.600	0.556	0.375	0.931	0.889
	C-2-1	4	0.071	1.14	6.645	0.234	0.284	0.459	0.221	0.680	0.803
	C-2-2	4	0.087	1.94	6.634	0.255	0.348	0.496	0.258	0.753	0.853
	C-2-4	4	0.153	4.33	6.667	0.253	0.612	0.614	0.380	0.994	0.727
Ref. 17	M-1	7	0.050	0.424	17.338	0.0975	0.329	0.231	0.248	0.479	0.51
	M-2	7	0.070	0.942	17.338	0.0975	0.528	0.282	0.346	0.628	0.64
	M-3	7	0.105	1.741	17.338	0.0975	0.742	0.329	0.426	0.755	0.80

5. CONCLUDING REMARKS

In this study, the behaviour and the load carrying capacity of steel box girders when the failure takes place in the stiffened compression flange are investigated both experimentally and theoretically. The emphasis was placed on the effects of the cross sectional area and the flexural rigidity of longitudinal stiffeners, and the yielding strengths of the plate and stiffeners upon the ultimate load carrying capacity of stiffened plates.

The following concluding remarks may be made from the foregoing discussions:

i) The ultimate load of stiffened plates under uniaxial compression may be empirically expressed by Eq. (29), and good correlation is found between the results from the formula and those from experiments.

ii) The load-deflection curve under the assumption of rigid plasticity may be given by Eqs. (22) and (23), and is considered to be the asymptote of the actual load-deflection curve of a stiffened plate.

iii) The ultimate load of stiffened plates is not necessarily determined from the linear buckling load.

iv) The ultimate load can be clearly found experimentally from Fig. 14, and it can also be found from Fig. 15 by taking the inflection point of $M_F/M_T - P_J$ (ratio of bending moment carried by the flange vs jack load) curve.

The following remarks may be added to the above concluding remarks:

a. The effect of the residual stresses was not investigated in the proposed theoretical formulations; however, it may be easily considered using tangent modulus. This effect nevertheless, may be implicitly considered in the formula of Eq. (29).

b. The effect of the torsional rigidity was not taken into account in the formula of Eq. (29); however, it may be considered with slight modification of the formula if sufficient number of tests are conducted.

ACKNOWLEDGEMENTS

The authors wish to express appreciation to Messrs. K. Nakamura, T. Miyata, and I. Toyoda for their help in the theoretical and experimental studies.

The experimental study was mainly sponsored by Sumitomo Metal Industries, Ltd. The numerical computation was performed by FACOM 230-

BIBLIOGRAPHY

- 1) Timoshenko, S.: Über die Stabilität versteifter Platten, Eisenbau, Bd. 12, 1921, S. 147-163.
- 2) Barbré, R.: Stabilität gleichmäßig gedrückter Rechteckplatten mit Längs-oder Quersteinen, Ing. Archiv, Bd. 8, 1937, S. 117-150.
- 3) Barbré, R.: Beulspannungen von Rechteckplatten bei gleichmässiger Druckbeanspruchung, Bauing., Bd. 17, 1936, S. 268-273.
- 4) Klöppel und Sheer: Beulwerte ausgesteifter Rechteckplatten, W. Ernst und Sohn, 1960.
- 5) Klöppel und Möller: Beulwerte ausgesteifter Rechteckplatten II, W. Ernst und Sohn, 1968.
- 6) von Karman, T., Sechler, E. E., and Donnell, L. H.: The strength of thin plates in compression, Trans. ASME, Applied Mechanics, Vol. 54, No. 2, 1932.
- 7) Timoshenko, S.: Theory of elastic stability, 2nd ed., McGraw-Hill Book Company, Inc., 1961.
- 8) Yoshiki, M.: Study on buckling and ultimate strength of hull structures, Naval Architecture and Shipbuilding in Japan, Vol. 75, 1953, pp. 85-109.
- 9) Dwight, J. B. and Moxham, K. E.: Welded steel plates in compression, The Structural Engineer, Vol. 47, No. 2, 1969, pp. 49-66.
- 10) Specification for the design, fabrication and erection of structural steel for buildings, AISC, 6th ed., 1966.
- 11) British Standards Institution: Specification for steel girder bridges, BS 153, Parts 3B & 4, 1972.
- 12) Light gage cold-formed steel design manual, AISI, 1962.
- 13) Japan Road Associations: Specifications for highway bridges, 1972.
- 14) Skaloud, M.: Post-critical behaviour of compressed webs uniformly reinforced by longitudinal stiffeners, Acier/Stahl/Steel, No. 4, 1964, pp. 187-192.
- 15) Skaloud, M.: The effect of an initial curvature on the post-critical behaviour of a uniformly compressed web reinforced by a longitudinal stiffener, Acier/Stahl/Steel, No. 5, 1965, pp. 241-246.
- 16) Maquoi, R. and Massonnet, Ch.: Non-linear theory of post buckling resistance of large stiffened box girders, Publ. IABSE, 31-II, 1971, pp. 91-140.
- 17) Dubas, P.: Tests about post-critical behavior of stiffened box girders, Report of the Working Commission, IABSE, Vol. 11, No. 3, 1971, pp. 367-379.
- 18) Ito, F. and Tajima, I.: Compressive tests of stiffened plates made of a high strength

- steel, Railway Technical Research Report, Japan National Railways, No. 313, 1962.
- 19) Ushio, M., Yoshikawa, O. and Komatsu, S.: An experimental study on ultimate strength of 80 kg/mm²-steel stiffened plates, Proc. JSCE, Vol. 218, 1973, pp. 31-37.
 - 20) Fukumoto, Y., Usami, T. and Okamoto, Y.: Ultimate compressive Strength of stiffened plates, ASCE Speciality Conference on Metal bridges, St. Louis, 1974.
 - 21) Hasegawa, A., Nagahama, M. and Nishino, F.: Buckling strength of stiffened plates under compression, Proc. JSCE, No. 236, 1975, pp. 1-14.
 - 22) Murray, N. W.: The behaviour of thin stiffened steel plates, Publ. IABSE, 33-I, 1973, pp. 191-201.
 - 23) Murray, N. W.: Buckling of stiffened panels loaded axially and in bending, The Structural Engineer, Vol. 51, No. 8, 1973, pp. 285-301.
 - 24) Sherbourne, A. N., Liaw, C. Y. and March, C.: Stiffened plates in uniaxial compression, Publ. IABSE, 31-I, 1971, pp. 145-177.
 - 25) Merrison Committee: Inquiry into the basis of design and method of erection of steel box girder bridges, Her Majesty's Stationary Office, London, 1973.
 - 26) Massonnet, Ch.: Tokyo seminar on some European contributions to the design of metal structures with emphasis on plasticity and stability, ultimate strength and optimum design of steel buildings, and steel plate and box girders, Nagoya University, 1974.
 - 27) Yamada, Y., Watanabe, E., Nakamura, K. and Miyata, T.: Postbuckling analysis of stiffened plates by finite element method, Proc. 9th Symposium on the Matrix Method for Structural Analysis and Design, JSSC, 1975, pp. 233-238.
 - 28) Haisler, W. E., Stricklin, J. A. and Stebbins, F. J.: Development and evaluation of solution procedures for geometrically nonlinear structural analysis by the Direct Stiffness Method, AIAAJ, Vol. 10, No. 3, 1972, pp. 264-272.
 - 29) Watanabe, E.: Postbuckling analysis of rectangular panels with flanges behaving elasto-plastically, Proc. JSCE, No. 220, 1973, pp. 117-130.
 - 30) Yamamoto, Y.: Elasticity and plasticity, Asakura Book Company (in Japanese, translated), 1961.
 - 31) Dorman, A. P. and Dwight, J. B.: Tests on stiffened compression plates and plate panels, International Conference on Steel Box Girder Bridges, ICE, London, 1973.
 - 32) Research Committee on Earthquake-Resistant Technology: Technical report on earthquake-resistant technology (in Japanese, translated), 1975.
 - 33) DIN 4114 Blatt 1: Stahlbau, Stabilitätsfälle (Knickung, Kippung, Beulung), Berechnungsgrundlagen, Vorshriften, 1959.
DIN 4114 Blatt 2: Stahlbau, Stabilitätsfälle (Knickung, Kippung, Beulung), Berechnungsgrundlagen, Richtlinien, 1953.

APPENDIX

Instrumentation

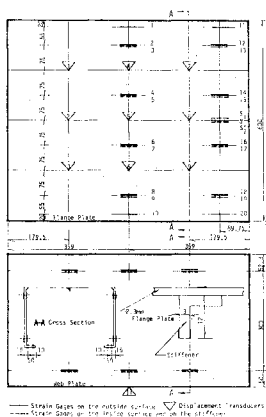


Fig. A.1 Instrumentation. Case 1.

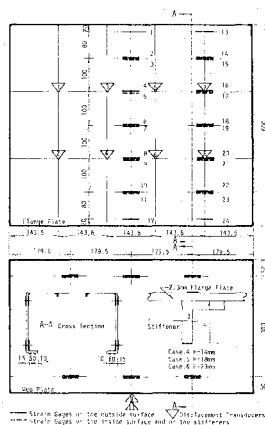


Fig. A.2 Instrumentation. Cases 4, 5, & 6.

(Received Sept. 25, 1975)